Modelling of a Nonlinear Swing Equation for a Non-salient Pole Rotor Synchronous Generator

Nor Syaza Farhana Mohamad Murad
Centre for Robotics and Industrial Automation (CeRIA)
Faculty of Technology and Electrical Engineering
Universiti Teknikal Malaysia Melaka (UTeM)
Melaka, Malaysia
p012110004@student.utem.edu.my

Muhammad Nizam Kamarudin
Centre for Robotics and Industrial Automation (CeRIA)
Faculty of Technology and Electrical Engineering
Universiti Teknikal Malaysia Melaka (UTeM)
Melaka, Malaysia
nizamkamarudin@utem.edu.my

Muhamad Fahezal Ismail
Centre for Water Engineering Technology
Water and Energy Section
Universiti Kuala Lumpur - MFI (UniKL MFI)
Bandar Baru Bangi, Selangor, Malaysia
fahezal@unikl.edu.my

Sahazati Md Rozali
Centre for Robotics and Industrial Automation (CeRIA)
Faculty of Technology and Electrical Engineering
Universiti Teknikal Malaysia Melaka (UTeM)
Melaka, Malaysia
sahazati@utem.edu.my

2024 IEEE 4th International Conference in Power Engineering Applications (ICPEA) | 979-8-3503-4457-8/24/$31.00 ©2024 IEEE | DOI: 10.1109/ICPEA60617.2024.10498450

***Abstract*—The simplification through linearization and neglecting damping power in the swing equation for a non-salient two-pole rotor degrades the accuracy and performance of the model. Thus, this paper presents the modelling of a nonlinear swing equation for a non-salient two-pole rotor of a synchronous generator via the direct phase method without neglecting the damping power. The functionality of the modelling is verified by comparing the obtained rotor angle graph via simulation in MATLAB/SIMULINK to the one obtained by a benchmarking paper. The simulation of the model proves that disturbance occurrences will perturb the rotor angle stability and might as well cause the rotor angle to operate at a new operating angle. Verification of this model allows it to be used in future studies of rotor angle stability analysis and enhancement.**

Keywords—synchronous generator, nonlinear swing equation, rotor angle stability, damping power

I. Introduction

Synchronous generators are essential components of power systems [1]. A stator, armature winding, rotor, field winding, and damper winding comprise a synchronous generator. According to the rotor structure, the synchronous generator is classified as a salient pole or a non-salient pole, also known as a cylindrical pole. The concentrated winding on the poles of the salient pole rotor caused non-uniform air gaps, resulting in non-uniform flux. The damper bars are located in the rotor poles to dampen rotor oscillation during rapid load changes. This rotor is intended for low- and medium-speed operation, as is common in hydroelectric power plants. A salient pole rotor has a large number of poles, a big diameter, and a small axial length. A non-salient pole rotor, on the other hand, has a single dispersed winding with a uniform air gap, resulting in uniform flux distribution. This rotor is intended for high-speed operation (1800rpm or 3600rpm), ideally driven by a steam turbine. This rotor features two or four poles, a small diameter, and a long axial length. The majority of substantial synchronous generators used non-salient pole rotor types with 150–1500MVA. Fig. 1 depicts the construction of both salient pole and non-salient pole rotors.

Modelling the synchronous generator is the most important part in modelling the power system because the stability of the power system is essentially dependent on the synchronism and operation stability of the synchronous generator [2], [3]. The power system's dynamic behaviour is primarily determined by the synchronous generator's dynamic performance [4]. The assumptions and simplifications given to the synchronous generator model affect the accuracy of power system analysis [3]. The power system model considered in this research is a single-machine infinite bus system in which one generator is connected to a major substation of a very large system through a transmission line. This model is very representative of the power system and is widely used in power system disturbance simulation [2].

Numbers of study recorded the employment of swing equation of synchronous generator for rotor angle assessment and enhancement. However, more studies considering salient-pole rotor rather than non-salient pole rotor [5]–[12]. Meanwhile, author in [13], employed nonlinear swing equation for non-salient pole rotor for assessment of rotor angle stability via particle swarm optimization (PSO) method. However, the damping power is neglected from the model. Knowing that damping power is an important function that minimizes the difference between two angular velocities, neglecting it is an impractical assumption. On the other hand, authors in [14]–[16] also employed the non-salient pole rotor swing equation in their enhancement studies. However, the swing equation is linearized which makes the stability studies only limited to small disturbances. These simplification and assumption made to the nonlinear swing equation degrades the accuracy and performance of the model. Thus, this research

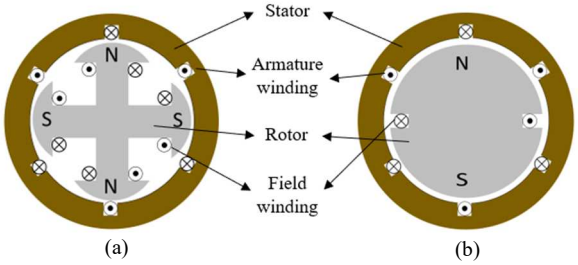

Fig. 1. (a) Salient pole rotor (b) Non-salient pole rotor

presents the modelling of nonlinear swing equation of non-salient two-pole rotor via direct phase modelling due to the capability of the model to simulate various loading conditions. The damping power is also taken into account.

II. Swing Equation

The swing equation is used to define the dynamic of the single-machine infinite bus system [17]. This swing equation is a nonlinear second-order differential equation [18]. The swing equation describes the relative motion of the rotor axis and the synchronously rotating stator field with respect to time. Under normal operating conditions, the relative position is fixed. However, during the disturbance, the rotor will either accelerate or decelerate with regard to the synchronously rotating air gap magneto motive force (MMF), resulting in relative motion. The relative motion produces a power angle between the rotor axis and the resulting magnetic field. To guarantee that the rotor angle is in an equilibrium state, the power angle must stay within the ideal range. The power angle in a steady system range between 20º to 30º. However, the generator can maintain synchronism up to a maximum power angle of 90º.

The power angle curve, as seen in Fig. 2, is a crucial component of a synchronous generator as it graphically depicts the generator's electrical output in relation to the power angle, where P_m is mechanical power, P_e is electrical power, P_{max} is maximum power, and δ_0 is initial power angle. A steady state condition for rotor angle stability is reached at the curve's intersection with P_m and δ_0. In this condition, P_m is equal to P_e, load angle, δ equal to δ_0, and rotor speed, ω_m synchronizes with synchronous speed, ω_{sm} . When P_e is within the range of the blue curve, P_m is considered to be larger than P_e , and ω_m is greater than ω_{sm} . The rotor accelerates as a result, increasing the load angle. The rotor will fluctuate about the δ_0 a few times and then settle back into steady state. P_m is said to be smaller than P_e, and ω_m is less than ω_{sm} when P_e is in the green curve range. The rotor will therefore slowdown in an effort to return to its steady condition. But as the red curve shows, if P_e is greater than P_{max} point, the rotor enters an unstable area where δ rises and never reaches δ_0.

Restoring the rotor to synchronous speed maintains the synchronous generator's stability. In the event that the disturbances do not cause a net change in power, the rotor resumes its regular operating state; if not, it works at a new power angle that corresponds to the synchronously spinning field [11]. If disturbances cause the rotor angle to vary, the synchronous generator's performance will be suffered.

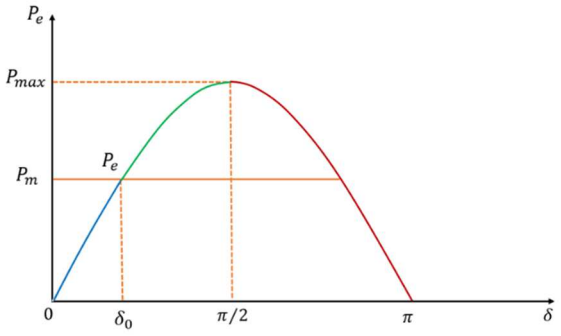

Fig. 2. Rotor angle curve

A. Modeling of Nonlinear Swing Equation

In order to analyze the stability problem of a non-salient two-pole rotor synchronous generator connected to an infinite bus, electrical power equation is substituted into swing equation, yielding

$$\frac{H}{\pi f_0}\frac{d^2\delta}{dt^2} = P_m - P_{max}\sin\delta \tag{1}$$

The swing equation is a nonlinear function of the power angle. Consider deviation, $\Delta\delta$ in power angle from initial operating point, δ_0, that is $\delta = \delta_0 + \Delta\delta$, the swing equation becomes

$$\frac{H}{\pi f_0}\frac{d^2\delta_0+\Delta\delta}{dt^2} = P_m - P_{max}\sin(\delta_0 + \Delta\delta) \tag{2}$$

Equation (2) can be extended as

$$\frac{H}{\pi f_0}\frac{d^2\delta_0}{dt^2} + \frac{H}{\pi f_0}\frac{d^2\Delta\delta}{dt^2} = P_m - P_{max}(\sin\delta_0\cos\Delta\delta + \cos\delta_0\sin\Delta\delta) \tag{3}$$

$P_{max}\cos\delta_0$ is the slope of the curve in the power angle graph at initial power angle, δ_0, which is also known as the synchronizing coefficient, denotes by P_s, the swing equation then becomes

$$\frac{H}{\pi f_0}\frac{d^2\delta_0}{dt^2} + \frac{H}{\pi f_0}\frac{d^2\Delta\delta}{dt^2} = P_m - P_{max}\sin\delta_0\cos\Delta\delta - P_s\sin\Delta\delta \tag{4}$$

During steady-state conditions, no current flows through the damper winding. However, when faults occur, eddy current is induced in the damper winding, which generates damping torque. The damping torque function is to minimize the difference between the two angular velocities. Damping power is approximately proportional to the speed deviation, as indicated in (5)

$$P_d = D\frac{d\delta}{dt} \tag{5}$$

If damping power is taken into account, the nonlinear swing equation becomes [19]

$$\frac{H}{\pi f_0}\frac{d^2\delta_0}{dt^2} + \frac{H}{\pi f_0}\frac{d^2\Delta\delta}{dt^2} - P_m + P_{max}\sin\delta_0\cos\Delta\delta + P_s\sin\Delta\delta + D\frac{d\Delta\delta}{dt} = 0 \tag{6}$$

The fault that occurs in the system is considered as power input, ΔP. Considering an increase in power input in the system, the nonlinear swing equation becomes

$$\frac{H}{\pi f_0}\frac{d^2\delta_0}{dt^2} + \frac{H}{\pi f_0}\frac{d^2\Delta\delta}{dt^2} - P_m + P_{max}\sin\delta_0\cos\Delta\delta + P_s\sin\Delta\delta + D\frac{d\Delta\delta}{dt} = \Delta P \tag{7}$$

In order to make (7) easier to compare with a standard second-order differential equation, $\frac{d^2\Delta\delta}{dt^2} + 2\zeta\omega_n\frac{d\Delta\delta}{dt} + \omega_n^2\Delta\delta$, it is divided by $\frac{H}{\pi f_0}$, which renders (8)

$$\frac{d^2\Delta\delta}{dt^2}+\frac{\pi f_0}{H}D\frac{d\Delta\delta}{dt}+\frac{\pi f_0}{H}P_{max}\sin\delta_0\cos\Delta\delta+\frac{\pi f_0}{H}P_s\sin\Delta\delta$$

$$=\frac{\pi f_0}{H}\Delta P-\frac{d^2\delta_0}{dt^2}+\frac{\pi f_0}{H}P_m \quad (8)$$

Let define state variables $[x_1,x_2]=[\Delta\delta,\dot{\Delta\delta}]$. Hence, first-order derivative of the state yields $[\dot{x_1},\dot{x_2}]=[x_2,\ddot{\Delta\delta}]$. Therefore, the nonlinear swing equation of the synchronous generator can be expressed as

$$\dot{x_1}=x_2$$

$$\dot{x_2}=-\frac{\pi f_0}{H}(P_{max}\sin\delta_0\cos x_1+P_s\sin x_1)-\frac{\pi f_0}{H}Dx_2+\frac{\pi f_0}{H}(\Delta P+P_m)-\frac{d^2\delta_0}{dt^2} \quad (9)$$

B. *Simulation of Nonlinear Swing Equation*

The simulation of the modeling is developed via MATLAB with Simulink toolbox version2021b software. The verification of the modelling is done by comparing the obtained result to the one obtained by the benchmarking paper chosen in [13]. The benchmarking paper modelled the nonlinear swing equation of a non-salient two-pole rotor via Fourier series expansion but neglected the damping power. The parameters of the synchronous generator are as tabulated in Table I [13]. The damping power is initially set at 0 p.u. as regard to the benchmarking paper for the purpose of model verification.

The fault occurrences in [13] is considered as benchmarking in this study as power input, ΔP but regarded in per unit (p.u.) value. In [13], the fault are at bus 1 with an impedance of j0.001p.u. to the ground, in the middle of the transmission line, and at bus 1 with zero to the ground impedance. Then, the fault in all three cases was cleared by removing the faulted line after 2.5 and 6.5 cycles.

III. Result and Analysis

For the first situation, in which the single-machine system experiences a three-phase failure at bus 1 with an impedance of j0.001p.u. to the ground, the simulation demonstrated that the most equivalent rotor angle graph is recorded when the fault value is 0.4p.u. When the fault is cleared at 2.5 and 6.5 cycles, a corresponding graph of rotor angle is obtained. Fig. 3 and Fig. 4 show the rotor angle graphs from the benchmarking study and this study, respectively.

TABLE I. Synchronous Generator Parameters

Symbols	Definition	Numerical Value
P_m	Real power	*0.6p.u.*
H	Inertia constant	*2.52 MJ/MVA*
V	Voltage at load terminal	*1.0p.u.*
f_0	Frequency	*60Hz*
δ_0	Initial rotor angle	*16.79°*
E	Voltage behind transient reactance	*1.1p.u.*
x'_d	Generator reactance	*j0.35p.u.*
X_1 and X_2	Transfer reactance	*j0.2p.u.*
D	Damping power	*0p.u.*
ΔP	Fault	*0.2–1.8p.u.*

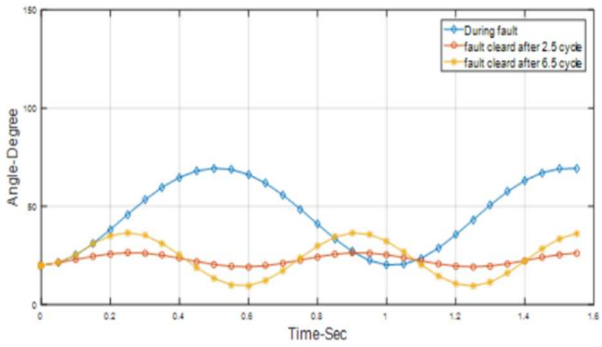

Fig. 3. Rotor angle graph for fault occur at bus 1 with an impedance of j0.001p.u to the ground

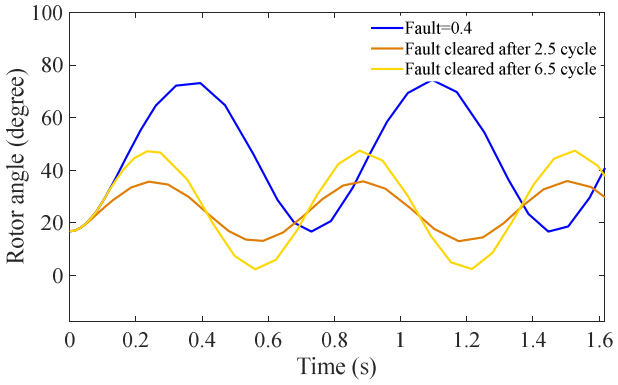

Fig. 4. Rotor angle graph for fault occur at 0.4p.u.

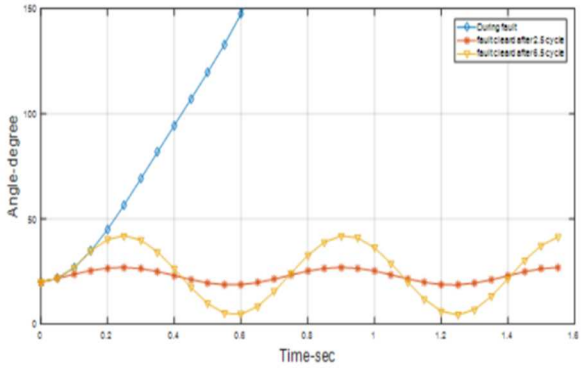

Fig. 5. Rotor angle graph for fault occur in the middle of transmission line

For the second case, in which the single-machine system encounters a three-phase fault in the middle of the transmission line, the simulation found that the most comparable graph of rotor angle is recorded when the value of fault is 0.63p.u.. Furthermore, the analogous graph of rotor angle is produced when the fault is cleared at 2.5 and 6.5 cycles. The graph of rotor angle of the benchmarking study and this study is as shown in Fig. 5 and Fig. 6, respectively. Comparing the second case to the first, a rise in the system fault causes the oscillation's amplitude to increase which increases the rotor angle.

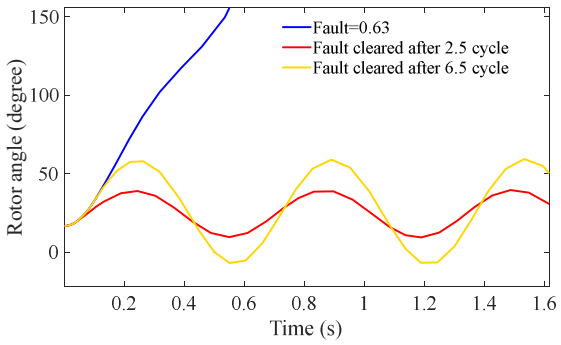

Fig. 6. Rotor angle graph for fault occur at 0.63p.u.

Then, the simulation indicated that the most comparable rotor angle graph is recorded when the fault value is 1.8 p.u. for the third scenario, in which the single-machine system encounters a three-phase fault at bus 1 with zero to the ground impedance. Additionally, a comparable graph of rotor angle is also obtained when the fault is cleared at 2.5 and 6.5 cycles. The rotor angle graphs from the benchmarking study and this study are shown in Fig. 7 and Fig. 8, respectively. In this case, it can be seen that a 1.8 p.u. fault occurrence in the system causes system instability. Implementation of fault clearing time after 6.5 cycles also resulted in unstable system performance. The system is back in synchronism if the fault is cleared at 2.5 cycles, but with a higher amplitude of oscillation compared to the previous cases.

The comparison of fault in paper [13] to power input, ΔP are tabulated in Table II. The simulation results with the three fault values of 04p.u., 0.63p.u., and 1.8p.u. verified the model

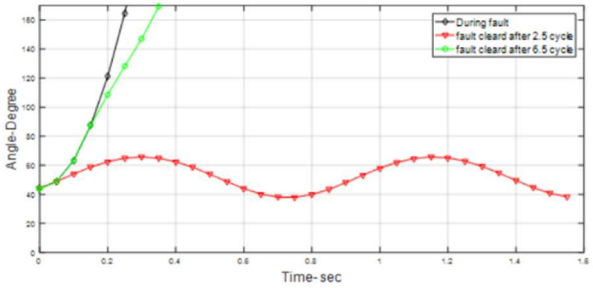

Fig. 7. Rotor angle graph for fault occur at bus 1 with zero to the ground impedance

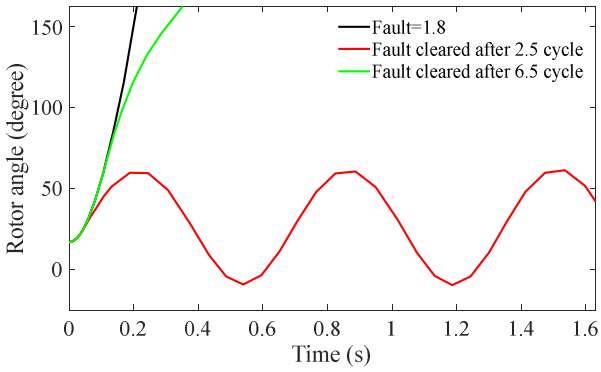

Fig. 8. Rotor angle graph for fault occur at 1.8p.u.

TABLE II. COMPARISON OF FAULT

Fault in paper [13]	**Power input, ΔP (p.u.)**
At bus 1 with an impedance of j0.001p.u. to the ground	0.4
In the middle of the transmission line	0.63
At bus 1 with zero to the ground impedance	1.8

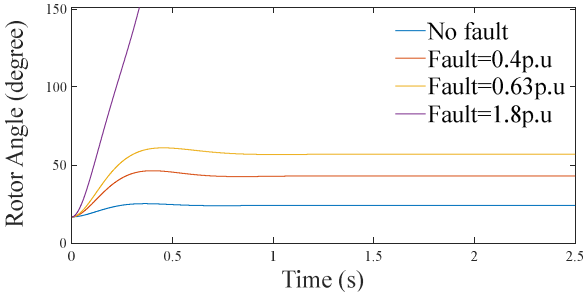

Fig. 9. Rotor angle for various fault

of the nonlinear swing equation of the non-salient two-pole rotor of synchronous generator developed in this study.

For stable systems, the graphs show sustained oscillation as damping power is not taken into consideration by setting it at 0p.u. Neglecting damping power is an impractical assumption that degrades the performance of the system; thus, damping power is added to the system (0.138p.u.). The graph of the rotor angle of various fault (without fault clearing time) is as shown in Fig. 9. It can be seen that damping power helps in decaying the oscillation. The graph shows the rotor angle begins at 16.79°, indicating the system's initial rotor angle. For the system with 0.4p.u. and 0.63p.u. fault, the rotor angle is still in stable condition (below 90°), but the operating angle have increases 26.196° and 40.206°, respectively. Whereas for the system with a fault value of 1.8 p.u., the rotor angle loses synchronism and never locks back into a stable rotor angle.

This proves that an increase in fault occurrences increases the rotor angle, which reduces its stability. Occurrences of fault will cause the rotor to operate at a new operating angle.

IV. CONCLUSION REMARKS

In this paper, a nonlinear swing equation is modelled for the non-salient pole rotor of a synchronous generator. The simulation result verified the functionality of the nonlinear swing equation of the non-salient pole rotor of a synchronous generator. The value of the fault effects the stability of the system, in which rotor angle stability decreases with the increment of the fault. For a system in which damping power is neglected, the rotor angle graph recorded sustains oscillation. Thus, it proves the impracticality of neglecting the damping power. The occurrence of damping power in the system results in reduced rotor angle oscillation. In the future, the verified model can be utilized for rotor angle assessment or enhancement studies.

ACKNOWLEDGMENT

We acknowledge the Ministry of Education Malaysia and Universiti Teknikal Malaysia Melaka (UTeM) for research facilities. This research also funded by research grant FRGS/1/2021/FKE/F00467.

REFERENCES

[1] J. Ritonja and B. Polajžer, "Analysis of synchronous generators' local mode eigenvalues in modern power systems," *Appl. Sci.*, vol. 12, no. 1, 2022, doi: 10.3390/app12010195.

[2] S. Luo, Y. Jian, and Q. Gao, "Synchronous generator modeling and semi - physical simulation," in Proc. 2019 22nd International Conference on Electrical Machines and Systems, ICEMS 2019, 2019, pp. 1–6, doi: 10.1109/ICEMS.2019.8921721.

[3] Yurika, Suwarno, G. H. Sianipar, and J. Naiborhu, "Modelling of synchronous generator for transient stability in power system," in Proc. 2nd International Conference on High Voltage Engineering and Power Systems: Towards Sustainable and Reliable Power Delivery, ICHVEPS 2019, 2019, pp. 125–129, doi: 10.1109/ICHVEPS47643.2019.9011059.

[4] N. Hatziargyriou, J. Milanovic, C. Rahmann, C. Canizares, D. Hill, and I. Hiskens, "Definition and Classification of power system stability - Revisited & extended," *IEEE Trans. Power Syst.*, vol. 36, no. 4, pp. 3271–3281, 2021, doi: 10.1109/TPWRS.2020.3041774.

[5] G. Tu, Y. Li, and J. Xiang, "Sliding mode control of energy storage systems for reshaping the accelerating power of synchronous generators," *IEEE Trans. Power Syst.*, vol. 38, no. 2, pp. 1242– 1256, 2023, doi: 10.1109/TPWRS.2022.3170703.

[6] H. Jiang and Y. Wang, "Power system transient stability enhancement using SMC controller under high wind power penetration scenarios," in Proc. 2020 2nd International Conference on Electrical, Control and Instrumentation Engineering (ICECIE), 2020, pp. 1–10, doi: 10.1109/ICECIE50279.2020.9309620.

[7] P. C. Papageorgiou and A. T. Alexandridis, "Stability and robustness enhancement of SGIB systems via angle estimation-based power controllers," in Proc. the 12th Mediterranean Conference on Power Generation, Transmission, Distribution and Energy Conversion (MEDPOWER 2020), 2020, pp. 491–496, doi: 10.1049/icp.2021.1281.

[8] M. Abubakar, B. Hussain, M. M. Majeed, and D. Ali, "Enhancement of rotor angle stability with superconducting fault current limiter," in Proc. 2022 International Conference on Recent Advances in Electrical Engineering & Computer Sciences (RAEE & CS), 2022, pp. 1–6, doi: 10.1109/RAEECS56511.2022.9954579.

[9] Y. Kumar, R. N. Mishra, and A. Anwar, "Enhancement of small signal stability of SMIB system using PSS and TCSC," in Proc. 2020 International Conference on Power Electronics & IoT Applications in Renewable Energy and its Control (PARC), 2020, pp. 102–106, doi: 10.1109/PARC49193.2020.236566.

[10] A. K. Hore, T. K. Roy, T. Sarkar, F. Faria, T. Haque, and M. M. Khatun, "Stability analysis of an SMIB power system using an integral backstepping-partial feedback linearizing approach," in Proc. 2021 International Conference on Automation, Control and Mechatronics for Industry 4.0 (ACMI), 2021, pp. 1–4, doi: 10.1109/ACMI53878.2021.9528265

[11] M. Rahim, "Methods to improve transient stability of low-inertia synchronous machines," in Proc. 2022 75th Annual Conference for Protective Relay Engineers, CPRE 2022, 2022, pp. 1–5, doi: 10.1109/CPRE55809.2022.9776599.

[12] A. Safavizadeh, E. Mostajeran, S. Ebrahimi, and J. Jatskevich, "Investigation of torque-angle characteristics of synchronous generators for transient stability analysis using equal area criterion," in Proc. 2022 21st International Symposium INFOTEH-JAHORINA (INFOTEH), 2022, pp. 16–18, doi: 10.1109/INFOTEH53737.2022.9751312.

[13] A. Zaidi and Q. Cheng, "An approximation solution of the swing equation using particle swarm optimization," in Proc. 2018 IEEE Conference on Technologies for Sustainability (SusTech), 2018, pp. 1–5, doi: 10.1109/SusTech.2018.8671355.

[14] K. Sunny, A. Sheikh, and S. Wagh, "Dynamic mode decomposition for prediction and enhancement of rotor angle stability," in Proc. 2020 7th International Conference on Control, Decision and Information Technologies (CoDIT), 2020, pp. 160– 165, doi: 10.1109/CoDIT49905.2020.9263893.

[15] J. J. Kim and J. H. Park, "A novel structure of a power system stabilizer for microgrids," *Energies*, vol. 14, no. 4, pp. 1–33, 2021, doi: 10.3390/en14040905.

[16] K. Charafeddine, Y. Ryzhkova, and Y. Matiunina, "Rotor angle stability of synchronous generator for power grid with wind energy," in Proc. 2021 International Conference on Industrial Engineering, Applications and Manufacturing (ICIEAM), 2021, pp. 147–151, doi: 10.1109/ICIEAM51226.2021.9446448.

[17] R. Ma, J. Li, J. Kurths, S. jie Cheng, and M. Zhan, "Generalized swing equation and transient synchronous stability with PLL- based VSC," *IEEE Trans. Energy Convers.*, vol. 37, no. 2, pp. 1428–1441, 2022, doi: 10.1109/TEC.2021.3137806.

[18] C. Andic, A. Ozturk, and B. Turkay, "Rotor angle stability analysis by using Lyapunov's direct method of a SMIB power system," in Proc. 2022 4th Global Power, Energy and Communication Conference (GPECOM), 2022, pp. 296–300, doi: 10.1109/GPECOM55404.2022.9815562.

[19] A. K. M. K. Hasan, M. H. Haque, and S. M. Aziz, "Damping rotor angle oscillations using battery energy storage systems," in Proc. *2020* IEEE International Conference on Power Electronics, Drives and Energy Systems (PEDES), 2020, pp. 1–6, doi: 10.1109/PEDES49360.2020.9379433.